WIND-WATER DRAG COEFFICIENTS OF LAKE ICE AT BREAKUP

by

Gee Tsang[1]

[1] Research Scientist, Ice and Hydraulics, Canada Centre for Inland Waters
Burlington, Ontario

ABSTRACT

The equation of motion of an ice field may be used as the theoretical basis for evaluating the wind drag coefficient and water drag coefficient over it. A field experiment on a lake at Spring breakup time based on such a theoretical basis gave a wind drag coefficient of 3.26×10^{-3} based on neutral wind velocity at 10 m height. This value is 2-3 times the values measured by other researchers over sea ice with other methods. The absorption of the form drag into the drag coefficient gives the seemingly large value. The above drag coefficient is for ice field with extensive telescoping and moving in direction perpendicular to the lines of telescoping. The great density gradient effect on the current distribution under a fresh water ice floe makes it impractical to relate the water drag coefficient to the current under the ice cover. By relating the water drag coefficient to the equivalent uniform current in the ice free part, the field experiment gave a drag coefficient of 5.85×10^{-2} to the ice field. This drag coefficient also takes both skin friction and form drag into account.

Key Words: Ice; water; air; drag coefficient; spring breakup; Lake.

RESUME

L'équation du mouvement d'un champ de glace peut servir de base théorique à l'évaluation du coefficient de traînée du vent et du coefficient de traînée de l'eau pour ce champ. Une expérience pratique effectuée d'après cette théorie sur un lac, au moment de la debâche du printemps, a donné un coefficient de traînée du vent de 3.26×10^{-3}, pour une vitesse du vent neutre à 10 m de hauteur. Cette valeur représente de 2 à 3 fois les valeurs trouvées par d'autres chercheurs sur les glaces de mer, au moyen de méthodes différentes. C'est parce que la traînée aérodynamique a été intégrée au coefficient de traînée que cette valeur est si grande en apparence. Le coefficient de traînée mentionné ci-dessus vaut pour un champ de glace où il y a un chevauchement considérable et un mouvement en direction perpendiculaire à celle du chevauchement. En raison de l'importance de l'effet du gradient de la masse volumique sur la répartition du courant sous un floe d'eau douce, il est difficile d'établir une relation entre le coefficient de traînée de l'eau et le courant de l'eau sous la couverture de glace. En établissant une relation entre le coefficient de traînée de l'eau et le courant uniforme équivalent dans la partie libre de glaces, l'expérience a donné un coefficient de traînée de 5.85×10^{-2} pour le champ de glace. Ce coefficient de traînée tient compte à la fois du frottement pelliculaire et de la traînée aérodynamique.

Mots clés: Glace;eau; air; coefficient de traînée; débâcle du printemps; lac.

INTRODUCTION

To calculate the movement of an ice field on a water body, the knowledge of the wind drag coefficient and the water drag coefficient on the ice field is essential. The wind drag coefficient on a sea ice floe was first measured by Untersteiner and Badgley (8). Other measurements of the wind drag coefficient on Sea ice of different surface conditions and at different geographic locations were made by Suzuki (7), Smith et al (6), Banke and Smith (1,2), Smith (5), Seifer and Langleben (4) and Langleben (3). In all the above studies except that by Suzuki, the wind drag coefficient was either calculated from the wind profile or from the turbulent velocity correlation. In Suzuki's study, the wind shear was directly measured by tensiometers.

Less was done on measuring the water drag coefficient of an ice field. Untersteiner and Badgley (8) were the only scientists who had made some water drag measurements on sea ice. Suzuki (7) suggested a way to measure the water drag coefficient but did carry out his suggestion.

In all the above studies, the ice floe was assumed stationary. The wind drag and the water drag were not measured simultaneously. So far, no study on the drag coefficients of wind and water on lake ice has been reported.

In the study reported here, the wind and water drag coefficients on a lake ice field at spring breakup time were measured. The measurements were made when the ice field was in motion. The wind drag coefficient and water drag coefficient were calculated simultaneously. These measured drag coefficients are compared with the drag coefficients obtained by earlier researchers.

BACKGROUND AND THEORY

An ice field may be approximately considered as a flat plate with a fully developed boundary layer. For the boundary layer, if the flow is neutrally stratified, the velocity distribution is given by the logarithmic law

$$V = \frac{1}{k} \left(\frac{\tau}{\rho}\right)^{\frac{1}{2}} \ln \left(\frac{z}{z_o}\right) \tag{1}$$

where k is the Von Karman constant and is generally accepted to have a value of 0.4, τ is the shear stress in the boundary layer, ρ is the density of the fluid, z is the distance from the boundary and z_o is called the roughness length of the boundary surface. According to the above equation, if the wind profile over an ice floe or the current profile under an ice floe under neutrally stable conditions is obtained, the plot of V versus ln z will be a straight line. The slope of the linear relationship will give $(\tau/\rho)^{\frac{1}{2}}/k$ while its intercept with the horizontal axis will give the boundary roughness length z_o.

Knowing the shear stress, the drag coefficient may be worked out from the following definition equation

$$C_z = \frac{2\tau}{\rho V_z^2} \tag{2}$$

where the subscript indicates the distance from the ice surface to the point where the velocity is measured and the drag coefficient is associated with.

The above theoretical basis was used by Untersteiner and Badgley (8), Seifert and Langleben (4) and Langleben (3). In their studies, a number of wind and current profiles were taken. From the logarithmic or nearly logarithmic profiles, either the drag coefficient or the roughness length were calculated.

Suzuki (7) measured the drag coefficient a little differently in that he measured the wind shear on a cut-off ice piece directly with tensiometers and the wind velocity at several heights. For the logarithmic winds, the roughness length and the drag coefficient were calculated directly from eqs (1) and (2) while treating the Von Karman constant as an unknown.

While the value of drag coefficient depends on the reference height, the boundary roughness length is free from such a restriction. However, C_z and z_o are simply related by

$$C_z = \frac{2k^2}{(\ell n\ (z/z_o))^2} \tag{3}$$

which is obtained by combining eqs. (1) and (2).

From boundary layer theory, the shear stress in a shear boundary layer is constant. For a fully developed boundary layer over an ice field, the shear stress is predominantly produced by turbulent momentum transfer. The molecular shear produced by viscosity is small and may be neglected from a practical point of view. The shear stress resulted from turbulent momentum transfer is given by

$$\tau = \overline{\rho v_1' v_3'} \tag{4}$$

where v_1' is the turbulent velocity in the main flow direction, v_3' is the turbulent velocity in the vertical direction and the bar above $v_1'v_3'$ means time-averaged value. Thus, by measuring the turbulent velocity correlations $\overline{v_1'v_3'}$, the shear stress on the ice floe may be evaluated. Knowing the shear stress and the mean velocity at one point, the drag coefficient and roughness length can be calculated from eqs. 1, 2 and 3. The wind drag coefficient on sea ice measured by Smith et al (6), Smith (5) and Banke and Smith (1,2) was obtained by the above method.

The drag coefficients of wind and ice on an ice field may also be measured from the movement of an ice field under known wind and current. For an ice field drifting on open water, if the time scale involved is small that the Coriolis effect may be overlooked, the equation of motion in the latitudinal direction is given by

$$\frac{1}{2} C_a \rho_a (V_{ax} - V_{ix})^2 - \frac{1}{2} C_b \rho_b (V_{ix} - V_{bx})^2 = \rho_i N T \frac{d^2 X_i}{dt^2} \qquad (5)$$

where C is the drag coefficient, ρ is the density, V is the velocity, X is the latitudinal displacement, t is time, N is the coefficient of virtual mass, T is the ice thickness and the subscripts a, b, i and x indicate air, water, ice and the latitudinal direction respectively. The writing of y for x in the above equation gives the equation of motion in the longitudinal (y) direction. In the above equation, the first term on the left is the wind shear on the ice, the second term is the drag by the water and the term on the right is the acceleration of the ice field. According to the above equation and its counterpart for the y direction, if the wind velocity, the current velocity, the ice velocity and acceleration and the ice thickness are measured at a given instant and a coefficient of virtual mass is assumed or experimentally obtained, the simultaneous solution of the two equations should give the wind and water drag coefficients of the ice field. Although theorectically speaking such an approach is correct, the motion of an ice field is more influenced by the accumulative effect of wind and current than their momentary value. The temporal and spatial fluctuation of the wind and current makes the selection of a representative wind and current difficult. The closing and widening of water gaps in the ice field and the sliding of telescoping ice floes also prevent the acceleration of the ice field to re-

spond instantaneously to the wind and current changes. The use of eq. 5 for drag coefficient evaluation therefore is impractical.

The above difficulty can be overcome if one tackles the problem from the integral approach. After all, for estimating the movement of an ice field over a water surface, one is more interested in the time-averaged value than the instantaneous value of the drag coefficients. By integrating eq. 5 twice with respect to time and rearranging the terms, one has

$$\iint_{t_o}^{t_1} (V_{ax}-V_{ix})^2(dt)^2 - \eta\iint_{t_o}^{t_1} V_{ix}^2(dt)^2 + 2\eta\iint_{t_o}^{t_1} V_{bx}V_{ix}(dt)^2$$

$$-\eta\iint_{t_o}^{t_1} V_{bx}^2(dt)^2 = \zeta\,(X_{i_1} - X_{i_o}) \qquad (6)$$

where

$$\eta = \frac{\rho_b C_b}{\rho_a C_a} \quad \text{and} \quad \zeta = 2\,\frac{\rho_i\, NT}{\rho_a\, C_a} \qquad (7)$$

If the wind, current and ice speeds in the time period of t_o to t_1 are known and the displacement of the ice field is measured, the integrals in eq. 6 can be evaluated and the equation contains η and ζ two unknowns only. If a similar equation is written for the y direction, the simultaneous solution of the two equations will give η and ζ. Knowing ζ, the wind drag coefficient Ca can be calculated from the second of eq. 7 with the measured ice thickness T and an assumed coefficient of virtual mass N. After Ca is obtained the water drag coefficient C_b can be calculated from η by the first of eq. 7.

The above approach provided the theoretical basis for the field experiment reported in this paper although the nature of the subsequent data

demanded some modification to the theory as will be seen later.

EXPERIMENT

SITE AND SITE PREPARATION - The field experiment was conducted on Lake Simcoe in Southern Ontario in the spring of 1974 and Big Bay Point was chosen as the study site. A number of bench marks along the shore were established as probable future survey stations. A grid of black dye was drawn on the ice cover (when the ice cover was strong) covering an area approximately 1350 m x 850 m. By inspecting the grid, the breakup, telescoping and deformation of the ice cover could be detected. Soundings were made over the experimental area which produced the bathymetric lines shown on Fig. 1. Thirteen marker flags atop timber tripods were erected on the ice cover along the outer perimeter of the grid at points 1 to 13. A meteorological tower was erected at the position shown on Fig. 1. Wind speed, direction, air temperature and humitity all at the height of 20 m above the lake surface, were measured at 5-minute intervals. A wind cup anemometer and a vane were used to measure the wind speed and wind direction. While the air temperature, humidity and wind direction were instantaneous readings, the wind speed was the average reading of the 5-minute sampling period. The current speed, direction and water temperature were measured by a string of 4 Geodyne self-recording current meters. The current meters were installed at the position shown on Fig. 1. Limnological data were sensed at the depths of 4m, 9m, 14m and 19m in a total depth of 21m. The current meter cable was tied to an anchor weight and maintained vertical by means of a float at the upper end. The float was 2 m from the under-surface of the ice cover. The limnological data were taken at 10-minute intervals. The current direction and water temperature were instantaneous readings but the current speed was the average reading of the 40-second sampling period.

Fig. 1

OBSERVATION - The break up of the ice cover began on April 14, 1974. In the morning of that day an intact ice cover was still completely covering the lake. At noon, the ice moved on shore and produced small ice piles (2m high) on the shore of the studied site. The ice was ripe, about 30-40 cm thick and has been considerably weakened by the mild weather of the past several days. The ice field moved to the other side the same night following the reversal of the wind direction and produced a major ice piling (8-10 m) on the opposite shore. An open water gap of 2 to 3 km wide at the western shore was created by the latter ice movement as shown by the aerial photograph Fig. 2, taken in the afternoon of April 16. The movement of the ice field caused the ice cover to break down into floes from hundred meters to several kilometers in linear dimension. Some telescoping and fingering of the neighbouring ice floes were seen. Visual observations from the air showed that as a result of telescoping and fingering, the surface area of the ice field was reduced by about 5 percent. A land inspection made at the opposite shore at noon on April 17 showed that the ice was ripe, without snow cover, smooth and showed the colour of the lake water. From the ice piles on the shore, columnar ice crystals could be clearly seen. The piled ice showed little strength, would disintegrate into crystals when forcefully kicked by foot. The ice sheet on the lake remained sufficiently strong for men to walk on. The ice sheet was about 30-40 cm thick. Where telescoping occurred, generally only two layers of ice were involved, however, in places ridges more than 1 m high were seen.

Fig. 2

The wind reversed its direction again in the morning of April 18 and drove the ice field to the experimental site. It was at that time the

drag coefficients of the ice field was measured. In less than 24 hours, the ice had deteriorated a great deal. For the part of the ice cover bordering the open water lead, many spots had even deteriorated into slush. The ice was so weakened that it broke up or even disintegrated instead of piling up when it hit the shore. Some telescoping of the ice sheet, however, was still observed. All the marker flags had toppled. Some were still visible by noting the upturned tripod legs but some had been lost from sight. Visual observation of the remaining markers showed that the ice field moved as a piece and there was no noticeable rotational motion of the ice field. The motion of the ice field, therefore, could be studied by the movement of one point.

As the ice field came to the visible range, simultaneous sightings of a selected marker from two visulally best bench marks (B.M. 8 and B.M. 13) were made with theodolites. Such a survey gave the movement of the ice field.

TREATMENT, ANALYSIS AND DISCUSSION OF EXPERIMENTAL DATA

MOVEMENT OF ICE FIELD - The geometric information relevant to the ice movement survey is shown on Fig. 3. As the ice field approached, angles ϕ and ψ were measured. The measured values of ϕ and ψ as functions of time are shown in Table 1 below:

Table 1

Figure 3

Based on the above values, smooth curves of ϕ and ψ versus time were plotted. By reading off the ϕ and ψ values from the curves at 5 minute intervals, the values of α and β and subsequently the coordinates of the marker x and y were calculated. The plotting of x and y versus time gives the lati-

tudinal and longitudinal displacements of the ice field as shown on Fig. 4a. From the displacement curves the velocity of the ice field in the latitudinal and longitudinal directions V_{ix} and V_{iy} were also calculated and plotted on Fig. 4a.

Figure 4

METEOROLOGICAL DATA - The wind speed and direction at the height of 20 m above the lake surface for the period just before and during the ice movement are shown on Fig. 4b. In Fig. 4b, the dashed lines are the recorded values and the solid lines are the approximated average curves. From the average wind speed and direction, the wind component in the x and y directions were calculated and plotted on Fig. 4a for comparison with the ice field velocity curves. It should be noted that in plotting Fig. 4a, th ice field is considered to have a positive velocity if it moved in the positive x and y directions while the sign convention for the wind is opposite to the above.

For a given wind velocity at a given height, the shear stress on a given surface is a function of the stability of the air. While an unstable stratification will encourage turbulent momentum transfer between layers, a stable stratification will inhibit it. The shear imparted by an unstable air stream on a surface therefore is higher than that by a stable air stream if the velocity at a characteristic point is the same. Because of the above, as mentioned in Instruction, some earlier researchers limited their experiments to neutral stratification conditions. For the study reported here multi-point wind measurements were not made. This makes it difficult to ascertain whether the stratification of the air was neutral during the experimental period. However, the air temperature in the experimental period was recorded to vary between 2.46 to 3.3°C with the mean value

to be approximately at 2.75°C. Assuming a 0°C surface temperature of the ice field and a linear temperature distribution between the ice surface and the sensing point at 20m, a temperature gradient of 0.138°C/m is obtained. Langleben (3) showed from his study that 86% of his neutral stability wind profiles were obtained when the temperature gradient was less than 0.15°C/m. Although whether or not the reverse is true has yet to be proved, there is some ground to assume a neutral stability wind profile at the time of the experiment. Langleben also showed that the wind profile is more likely to be logarithmic when the wind gradient is small. For his study, 85 percent of his neutral stability winds occurred when the velocity gradient was less than 0.5 ms^{-1}/m based on wind velocities measured at 1 m and 2 m levels. For the study here, Fig. 4 b shows that during the experimental period the wind was at the most about 1.25 m/s at 20 m. The velocity gradient at 1.5 m (midpoint of 1m and 2 m levels) should be much smaller than 0.5 ms^{-1}/m. The neutral wind profile assumption therefore finds another favourable support. In summarizing, one may say that if the wind was not neutral, it should not be too far away from it. The temperature difference between the ice cover and the air might cause a slightly stable stratification and consequently a slightly lower drag, but such effects should not be significant. The wind speed curve on Fig. 4b also supports the above argument. It is seen from the dashed line that the fluctuation of the wind was about 10 to 15 percent of the mean flow velocity, a generally expected figure of the turbulence level of a neutrally stratified wind.

During the experimental period, the relative humidity of the air was measured to vary from 63 to 67 percent. Banke and Smith (1) showed that for an air temperature of 3°C, even a change in relative humidity of as much as 50 percent will not significatly affect the stability of the air.

The humidity data, therefore, were not considered as useful data in the study.

LIMNOLOGICAL DATA - The upper two current meters failed to work at the time of ice movement. The uppermost current meter had never worked and the second current meter broke down 8 days before the ice movement. The current speed, direction and water temperature obtained by the bottom two current meters during the experimental period are shown on Fig. 5.

Figure 5

It is seen from Fig. 5 that at the time of spring break up, the lake water was stably stratified and the lake currents showed strong layering effects. The current at 14 m and the current at 19 m deep, although only 5 m apart, flowed nearly in opposite directions. This stable stratification and layering effect were not accidental. The analysis of the limnological data for periods when the second current meter from the top was still working showed that a stable temperature gradient existed in the water for the whole ice covered period and the layering effect extended at least from the bottom to the second current meter at the 9 m depth and very probably extended right to the water surface.

The lack of current data for the upper layers of the lake makes it difficult to calculate the water drag on the ice field. In fact, it is questionable whether the knowledge of the upper currents would be of much help to water drag calculation. Because of the temperature gradient, the current under the ice would not be logarithmic even if the direction did not vary with depth. Not knowing the functional form of the current profile, the use of eq. 2 for drag or drag coefficient calculation becomes senseless.

The above difficulty may be overcome by introducing the concept of an equivalent uniform approaching current, which is a uniform current of

neutral stability approaching the upstream edge of the ice field and producing the same drag to the underside of the ice. The introduction of such a concept is rational because the concept of drag was first developed for submerged bodies in a uniform flow. For a submerged flat plate of limited size, the equation for calculating the drag force on one side is

$$\text{Drag} = \text{Area of plate} \times \frac{1}{2} \rho C V^2 \tag{8}$$

The modification of the above equation to eq. 2 for calculating the shear stress in the fully developed boundary layer of an infinite plate is permitted only because for a current of given stability, the velocity at a given point in the boundary and the uniform velocity of the approaching current are one to one corresponded. By considering V_{bx} and V_{by} as the velocity components of the equivalent uniform current in the ice free part of the lake, one thus can still use eq. 6 for calculating the water and air drag coefficients.

It is seen from Fig. 5 that in the experimental period of ice movement, the currents at 14 m and 19m depths varied with time. Therefore, strictly speaking, the equivalent uniform approaching current should also be a function of time. However, since the variation in speed and direction of the lake currents as shown by Fig. 5 was limited and since one is more interested in the average effect of the water drag rather than the momentary effect V_{bx} and V_{by} may be considered as constants for the experimental period and be brought out of the integral sign of eq. 6. Eq. 6 then can be further reduced to

$$\iint_{t_o}^{t_1} (V_{ax}-V_{ix})^2 (dt)^2 - \eta \iint_{t_o}^{t_1} V_{ix}^2 (dt)^2 + 2\eta V_{bx} \iint_{t_o}^{t_1} V_{ix} (dt)^2$$

$$- \frac{1}{2} \eta V_{bx}^2 (t_1^2 - t_o^2) = \zeta (X_{i_1} - X_{i_o}) \tag{9}$$

A similar equation can be written for the longitudinal direction.

With the field data collected, the integrals in the above equation can be evaluated and an equation containing 4 unknowns ζ, η, V_{cx} and V_{cy} will result. If the experimental period is properly divided, then 4 equations for different time intervals can be obtained and their simultaneous solution will give the values of the 4 unknowns.

EVALUATION OF DRAG COEFFICIENTS AND EQUIVALENT CURRENT

According to the discussions given in the above section, it appears to be natural to divide the experimental period into two intervals and write eq.9 and its longitudinal counterpart for each interval for obtaining the four required equations. However, this approach was not chosen because first of all such a division will lead to high order (4th power) polynominal equations for final evaluation of the unknowns and their solution involves lengthy computer programming. Secondly, it is seen from Fig. 4a that the longitudinal velocity of the ice field showed great variation. Because the presence of water gaps in the ice field and the telescoping of neighbouring ice floes, part of the wind shear would be used for internal deformation of the ice field instead of for its macroscopic movement during the velocity varying time. The use of such data in an equation describing the average motion of the ice field therefore would introduce error, especially when the time period concerned is short and the momentary internal deformation effect is more felt. Large velocity change in the latitudinal direction are not shown by Fig. 4a except for the initial moment of the experimental period. The effect of the wind shear therefore would be mostly shown by the movement of the ice field. The field data in the latitudinal direction thus are more appropriate for use in the equation of motion. In addition, the use of the higher wind and current

velocities in the latitudinal direction also means that for the same instrumentation and human error, less relative effect will be felt.

Based on the above reasons, the latitudinal data were used for evaluating the drag coefficients. Since Eq. 9 contains 3 unknowns η, ζ and V_{bx}, 3 independent equations of the form of eq. 9 were written three differen time intervals of t_o - (t_o + 20.0) min.; t_o - (t_o + 40.0) min. and t_o - (t_o + 62.5) min., where t_o = 1108.75 hr, E.S.T. The integrals in the equations were evaluated numerically with 2.5 min. time increments. The simultaneous solution of the three equations gave the following rational roots;

$$V_{bx} = -8.64 \text{ cm/s}, \quad \eta = 1.57 \times 10^4 \quad \text{and} \quad \zeta = 1.79 \times 10^7 \text{ cm}$$

The longitudinal component of the equivalent uniform approaching current V_{by} was calculated from the complementary equation to eq.9 in the Y direction. The equation was written for the whole experimental period of t_o to (t_o + 62.5) min. based on the reasoning that the compression effect on the ice field due to acceleration during the early part of the period would be compensated by the loosening effect during the later deceleration part of the period (See the V_{iy} curve on Fig. 4 a). Again the integrals in the equation were evaluated numerically with 2.5 min. time increments. After substituting the values of η and ζ shown above into the quadratic equation, two roots of V_{by}

$$V_{by} = - 7.61 \text{ cm/s and } V_{by} = - 5.03 \text{ cm/s}$$

were obtained. Both roots appear rational although the physical event required only one root. However, the selection of either root would not introduce much difference to the total velocity. When the first root of V_{by} is

chosen, the total speed of the current is 11.5 cm/s and when the second root is chosen, the total speed is 10.0 cm/s. For the study here, the exact value of the equivalent uniform approach current is not important for it only serves to indicate the magnitude of the current at which the drag coefficient was measured.

Knowing η and ζ, the air and water drag coefficient can be calculated from eq. 7. With a density of water of 1000 kg/m^3 and a density of air of 1.3 kg/m^3 at 0°C, the ratio of C_b/C_a is calculated from the first of eq. 7 to be

$$C_b/C_a = 20.5$$

The calculation of the wind drag coefficient C_a from the second of eq. 7 requires the knowledge of ice thickness T and the coefficient of virtual mass N. The ice thickness was not measured at the time of the experiment. But as shown in OBSERVATION the ice thickness was measured about 24 hours earlier to be 30-40 cm. Since the breakup of an ice cover involves the ripening, candling and disintegration of the ice rather than the gradual thinning of it, an ice thickness of 30 cm at the time of the experiment may be reasonably assumed. The exact value of the coefficient of virtual mass is difficult to estimate for it not only depends on the boundary roughness of the ice field, but the stability condition of the water also. The stabler the stratification, the less will be the momentum exchange between the layers and a smaller value for N. The value of N for a circular cylinder in a uniform, neutrally stratified flow is 2. For elliptical cylinders of different axial ratios, the value of N has been found to lie between 1 and 2 when the long axis is parallel to the flow. For the ice field in question, a value of 1.2 may be assumed in absence of a better estimate. With

the above values of T and N and an ice density of 920 kg/m^3, the wind drag coefficient is calculated from the second of eq. 7 to be

$$C_a = 2.85 \times 10^{-3}$$

The water drag coefficient C_b is calculated with the above value of C_a to be

$$C_b = 5.85 \times 10^{-2}$$

DISCUSSIONS

Knowing the wind drag coefficient, the roughness length of the upper ice surface may be calculated from eq. 3 which now is rearranged as

$$z_o = z \; e^{-k\sqrt{\frac{2}{C_z}}} \qquad (10)$$

The substitution of $z = 2000$ cm, $k = 0.4$ and $C_z = C_a = 2.85 \times 10^{-3}$ into the above equation gives

$$z_o = 0.0824 \quad \text{cm}$$

In the earlier works quoted, the wind drag coefficients were all referred to 10 m height wind speeds. The relationship between wind drag coefficients based on different reference heights can be shown from eq. 3 to be

$$C_{a,z_1} = 2 \left[\left(\frac{2}{C_{a,z_2}} \right)^{\frac{1}{2}} - \frac{\ell n(z_2/z_1)}{k} \right]^{-2} \qquad (11)$$

where z_1 and z_2 are two reference heights. The substitution of z_1 = 10 m z_2 = 20 m and $C_{a,z_2} = C_{a,20} = 2.85 \times 10^{-3}$ into the above equation gives

$$C_{a,10} = 3.26 \times 10^{-3}$$

The roughness length and the wind drag coefficient for 10 m wind shown above may now be compared with the values measured by earlier researchers as shown on Table 2.

Table 2

It is seen from Table 2 that the wind drag coefficient obtained in this study is greater than those obtained by the earlier researchers by a factor of 2 to 3. At first glance, one may have the impression of an unusually large wind drag coefficient for a lake ice cover. However, this is not the case because the drag coefficients measured by the other researchers are for the skin shear in the boundary layer only while the drag coefficient measured in this study is the overall drag coefficient of the ice field accommodating both the skin friction and the form drag caused by the surface irregularities. Banke and Smith (2) in their study showed that for ridges 1 m high and at a density of 5 ridges/km, the form drag caused by them may add an equivalent drag coefficient of 1.5×10^{-3} to the skin drag coefficient. In this study , although ridges higher than 1 m were few, the ice field was heavily telescoped and the telescoped parts projected easily 50 cm into the air. The density of telescoping was not measured but visual estimate showed that 5 telescoping/km would not be unreasonable. The roughening of the ice surface as a consequence of breaking and compression of the ice floes also tended to give a higher skin friction drag coefficient. A drag coefficient of 3.26×10^{-3} therefore is in line with the earlier values. One must bear in mind, however, that the drag coefficient

obtained in the study is only good for an ice field in spring breakup time and that extensive telescoping had taken place between ice floes. Strictly speaking, the drag coefficient is only good for fresh water ice of 30-40 cm thick because for sea ice or fresh water ice of different thickness the ice floes may break and telescope differently and hence give different surface irregularities. The drag coefficient is for an ice field moving with the telescoping lines normal to the wind. If the direction of movement is 90 degrees from the above, about half the value of the measured drag coefficient should be used. No parallel discussion on the roughness length will be made here since it will not add new information to what has been said.

As mentioned earlier in the paper, the water drag coefficient under an ice cover so far has only been measured by Untersteiner and Badgley (8). From measuring the current profile under a sea ice cover and analysing the logarithmic profiles, they obtained an average roughness length of 2 cm. With this roughness length, the water drag coefficient for a reference current velocity at different heights can be calculated from eq. 3 to be

z	1	2	3	4	5 m
$C_{b,z}$	2.0×10^{-2}	1.49×10^{-2}	1.22×10^{-2}	1.09×10^{-2}	1×10^{-2}

Although the above drag coefficients are of the same order of magnitude as the drag coefficient of 5.85×10^{-2} obtained in the reported study, they are not comparable. The former drag coefficients are for a logarithmic current profile while the latter is for an equivalent uniform approaching current or the uniform current in the ice free water. Under a sea ice cover, a neutral logarithmic current profile is possible because the convective motions set up by the rejection of brine during the freezing process tend to destroy any density gradient that may exist under the ice cover. For fresh

water ice, such a natural convection mechanism does not exist so the current below will hardly be logarithmic. In fact, it will also likely be non-unidirectional as shown in the study. For the above reasons, the sea ice drag coefficients would have little use for a fresh water ice field and the analysis of the velocity profile under a fresh water ice sheet for evaluating the drag coefficient or to relate the drag coefficient to the velocity at one point becomes senseless.

The use of a drag coefficient associated with the equivalent uniform approaching current seems rational. First, it is easy to measure the current in an open water. Secondly, the current in the open part of a lake has a high probability of being uniform especially if the water expanse is wide and the weather is windy. The turbulence produced by the wind shear encourages momentum transport between layers and this leads to a uniform current for the upper layers, if not for the whole depth. The drag coefficient obtained in this study therefore is of practical value.

The reported field study, at best, gave only one measurement of the wind and water drag coefficients under on particular set of test conditions. Their indiscriminated use therefore should be avoided. More experiments should be done to give the values of C_a and C_b under different field conditions.

Although different methods have been used to evaluate the wind and water drag coefficients of an ice cover and the method reported in this paper is not the easiest for drag coefficient evaluation, it has the advantage of giving a drag coefficient for the whole ice field instead of at one sampling point alone. It also has the advantage of obtaining the wind and water drag coefficients simultaneously when the ice field is in motion, a situation when their knowledge is most needed. In addition, the drag

coefficients so obtained take into account both the skin friction and the form drag by the irregularities of the ice cover while for the other methods a separate effort has to be made to evaluate the form drag after the skin shear is obtained.

CONCLUSIONS

The study shows that the wind and water drag coefficients of an ice field can be calculated from the wind data and the movement of the ice field. The knowledge of the current under the ice field is not necessary for evaluating the water drag coefficient of a fresh water ice field. The drag coefficient based on the equivalent uniform approaching current or the uniform current in the open part of the lake has a wider rational basis and is more useful in calculating the movement of an ice field.

The measured wind drag coefficient of 3.26×10^{-3} based on neutral wind at 10 m is in line with earlier measurements over sea ice by other researchers if the effect of form drag is included. This drag coefficient may be used for lake ice cover at Spring breakup time after extensive telescoping has taken place and the ice moves in the direction perpendicular to the telescoping lines. For earlier ice and for movement in other direction, the ice field will be smoother to the wind and give a smaller drag coefficient.

The water drag coefficient of 5.85×10^{-2} is the only measured value known to exist for a fresh water ice field. This drag coefficient should be used in conjunction with the uniform current at the upstream edge of the ice field. The study shows that the water drag coefficient obtained for a sea ice cover may not be used for a fresh water ice cover because the current under the fresh water ice is much more complicated than that under the sea ice.

APPENDIX I. - REFERENCES

1. Banke, E.G. and Smith, S.D., "Wind Stess Over Ice and Over Water in Beaufort Sea", J. of Geophysical Res., Vol. 76, No. 30, Oct. 1971, pp. 7368-7374.

2. Banke, E.G. and Smith, S.D., "Wind Stress on Arctic Sea Ice", J. of Geophysical Res., Vol. 78, No. 33, Nov. 1973, pp. 7871-7883.

3. Langleben, M.P., "A Study of the Roughness Parameters of Sea Ice from Wind Profiles", J. of Geophysical Res., Vol. 77, No. 30, Oct. 1972, pp. 5935-5944.

4. Seifer, W.J. and Langleben, M.P., "Air Drag Coefficient and Roughness Length of a Cover of Sea Ice", J. of Geophysical Res., Vol. 77, No. 15, May 1972, pp 2708-2713.

5. Smith, S.D., "Wind Stress and Turbulence over a Flat Ice Floe", J. of Geophysical Res., Vol. 77, No. 21, July 1972, pp. 3886-3901.

6. Smith, S.D., Banke, E.G. and Johannessen, O.M., "Wind Stress and Turbulence over Ice in the Gulf of St. Lawrence", J. of Geophysical Res., Vol. 75, No. 15, May 1970, pp. 2803-2812.

7. Suzuki, Y., "Wind and Water Drag of an Ice Floe", Proc. Int. Conf. on Physics of Snow and Ice, Aug. 1966, Sapporo, Japan, Vol. 1, Part 1, pp. 661-666.

8. Untersteiner, N. and Badgley, F.I., "The Roughness Parameters of Sea Ice", J. of Geophysical Res., Vol. 70, No. 18, Sept. 1965, pp. 4573-4577.

APPENDIX II - NOTATION

The following symbols are used in this paper:

C = drag coefficient;

C_z = drag coefficient at z;

C_a = wind drag coefficient;

C_b = water drag coefficient;

C_{a,z_1} = wind drag coefficient for reference wind at height z_1;

C_{a,z_2} = wind drag coefficient for reference wind at height z_2;

$C_{a,10}$ = wind drag coefficient for reference wind at 10 m height;

$C_{b,z}$ = water drag coefficient for reference current at depth z;

k = Von Karman constant;

N = coefficient of virtual mass;

T = Thickness of ice;

t = time ;

t_o, t_1 = beginning instant and terminating instant of a time period;

V = velocity;

V_z = velocity at z;

V_{ax} = wind speed in the latitudinal direction;

V_{ix} = speed of ice field in the latitudinal direction;

V_{bx} = current speed in the latitudinal direction;

V_{by} = current speed in the longitudinal direction;

v_1' = turbulent velocity in the direction of flow;

v_2' = turbulent velocity in the direction normal to the mean flow;

$\overline{\rho v_1' v_2'}$ = time averaged value of $PV_1'V_2'$;

X_i = latitudinal position of ice field;

X_{io} = latitudinal position of ice field at time t_o ;

X_i = latitudinal position of ice field at time t_i;

z = vertical distance from the ice surface;

z_o = roughness length of ice surface;

z_1, z_2 = two reference heights;

$\eta = \frac{\rho_b C_b}{\rho_a C_a}$;

$\zeta = \frac{2\rho_i NT}{\rho_a C_a}$;

ρ = density;

ρ_a, ρ_b, ρ_i = density of air, water and ice respectively;

ϕ, ψ = angle between baseline and sighting line as defined by Fig. 3;

τ = shear stress;

Captions of Tables and Figures:

Figure 1 Experimental Lake and Site

Figure 2 Ice Field before Experimental Movement

Figure 3 Ice Movement Survey Arrangement

Figure 4 Displacement and Velocity of the Ice Field and the Associated Wind

Figure 5 Limnological Data at Time of Ice Movement

Table 1 Measured Values of ϕ and ψ

Table 2 Comparison of Roughness Lengths and Wind Drag coefficients by different Researchers.

Summary:

A field experiment involving collecting meteorological and limnological data and measuring the movement of an ice field gave a wind drag coefficient of 3.26×10^{-3} and a water drag coefficient of 5.85×10^{-2} to a lake ice field at spring breakup time.

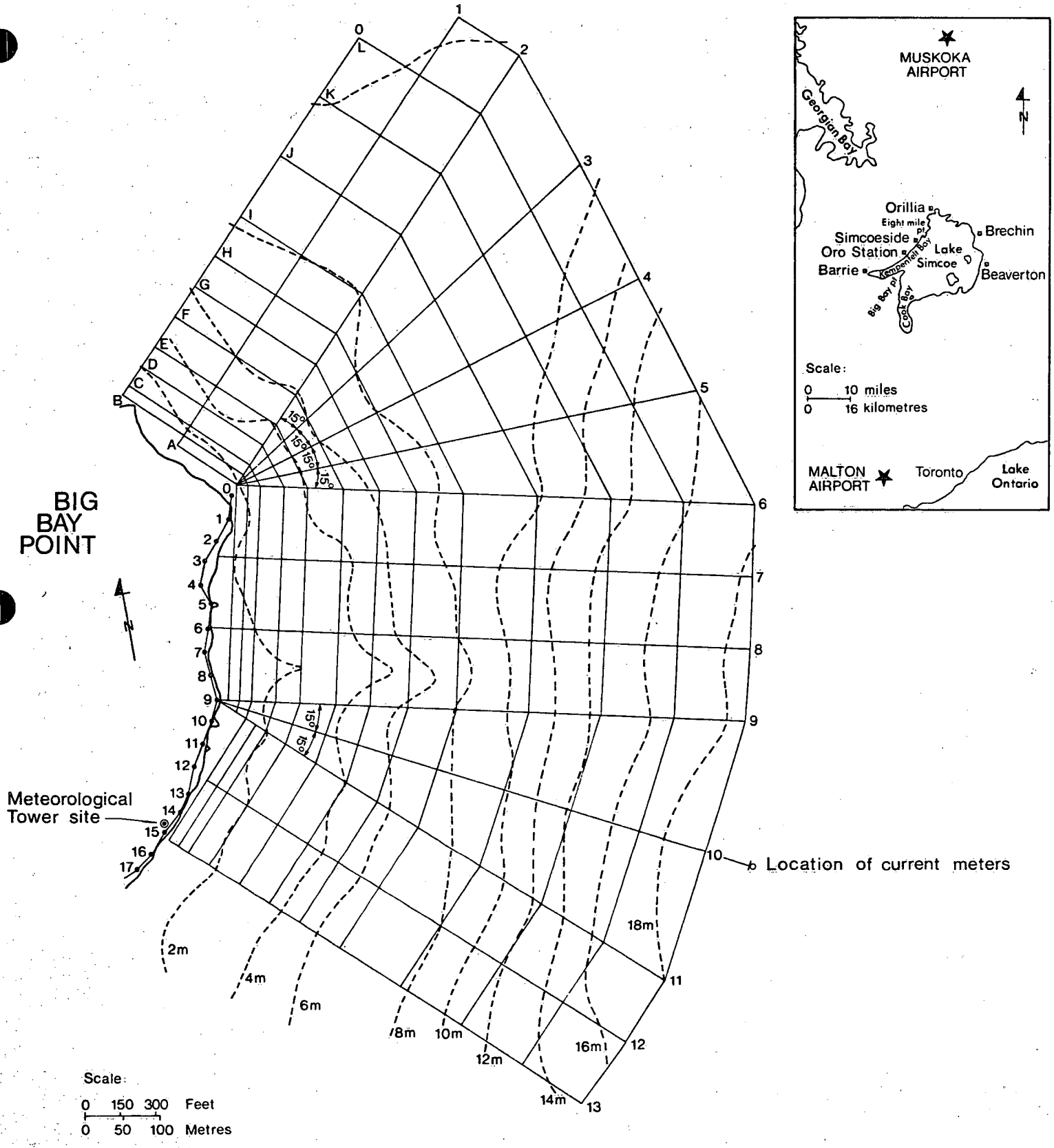

Fig.1 EXPERIMENTAL LAKE AND SITE

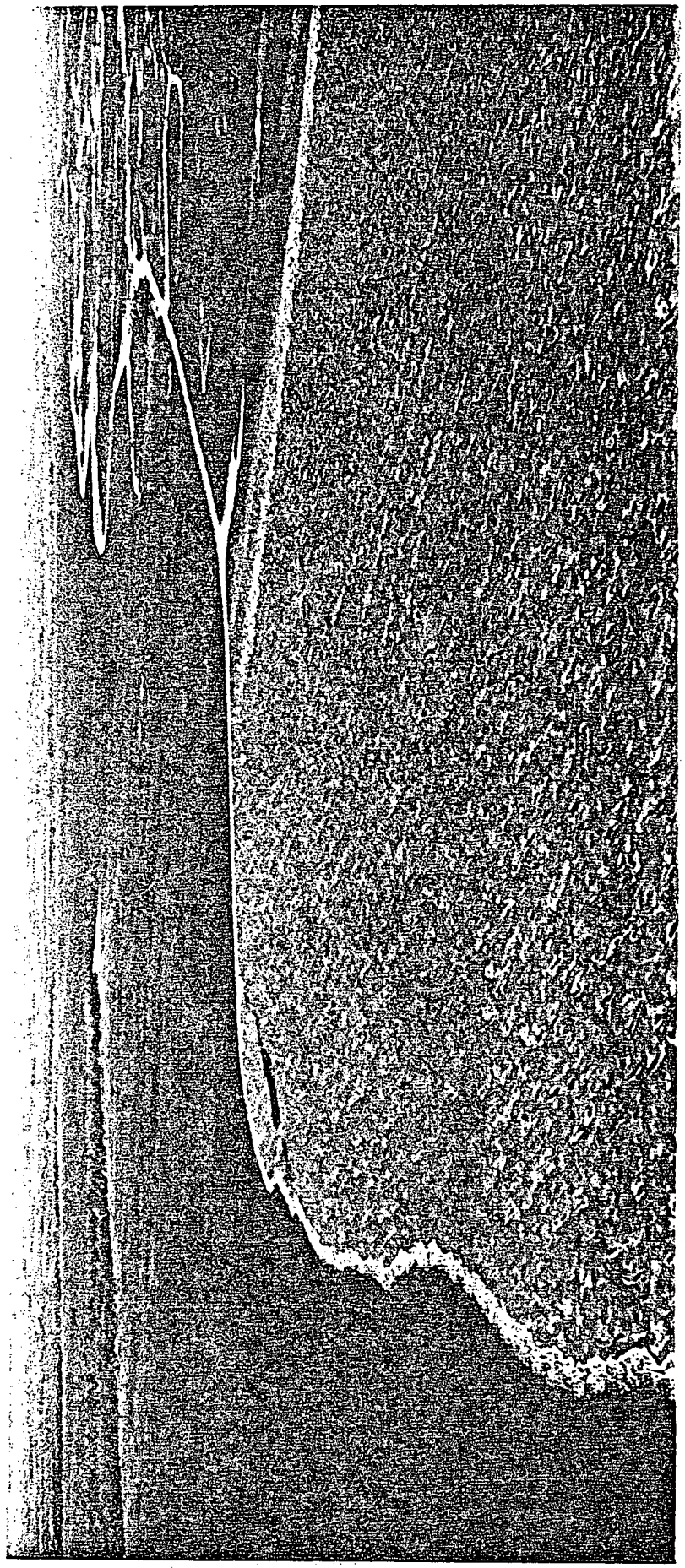

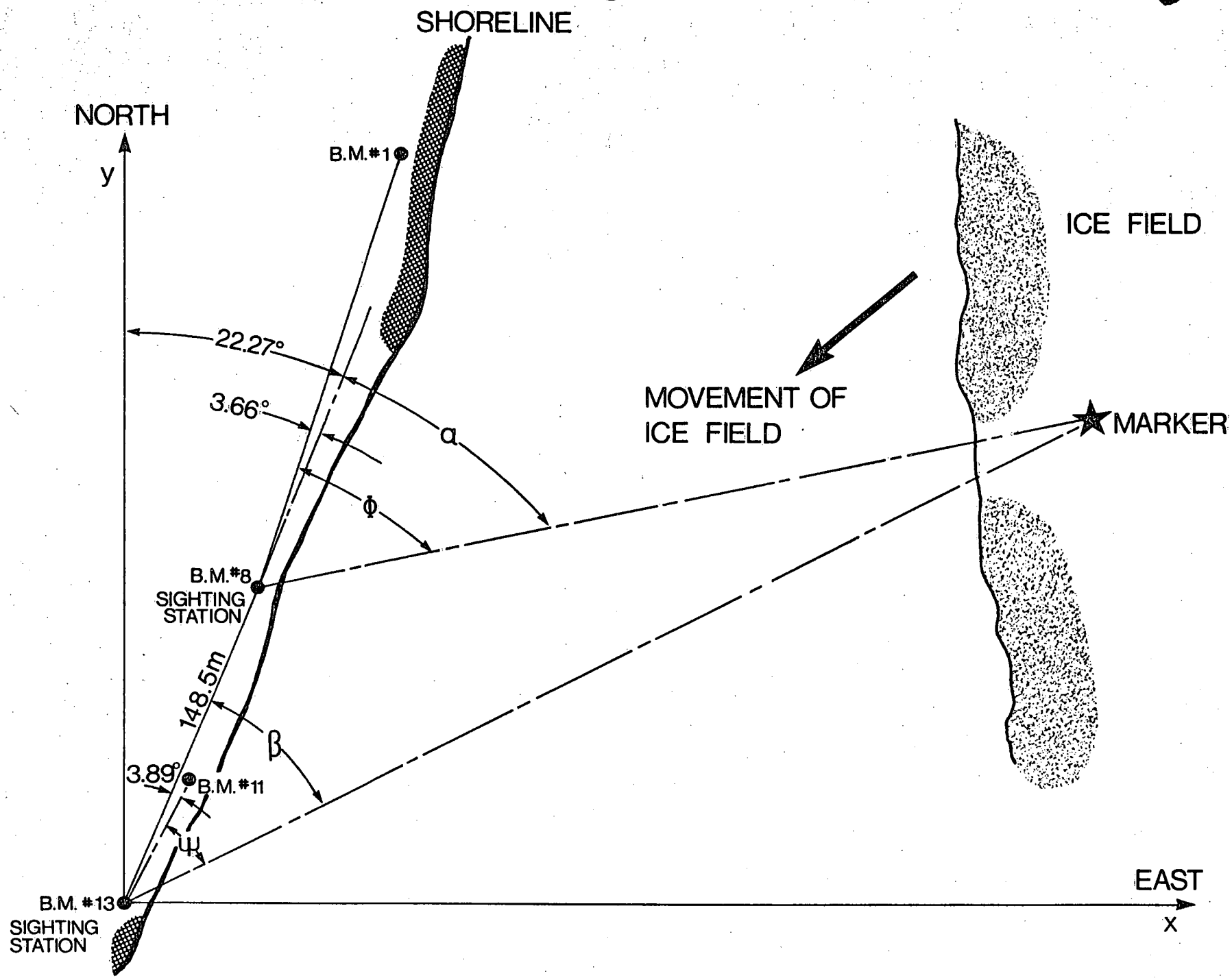

FIG. 5 ICE MOVEMENT SURVEY ARRANGEMENT

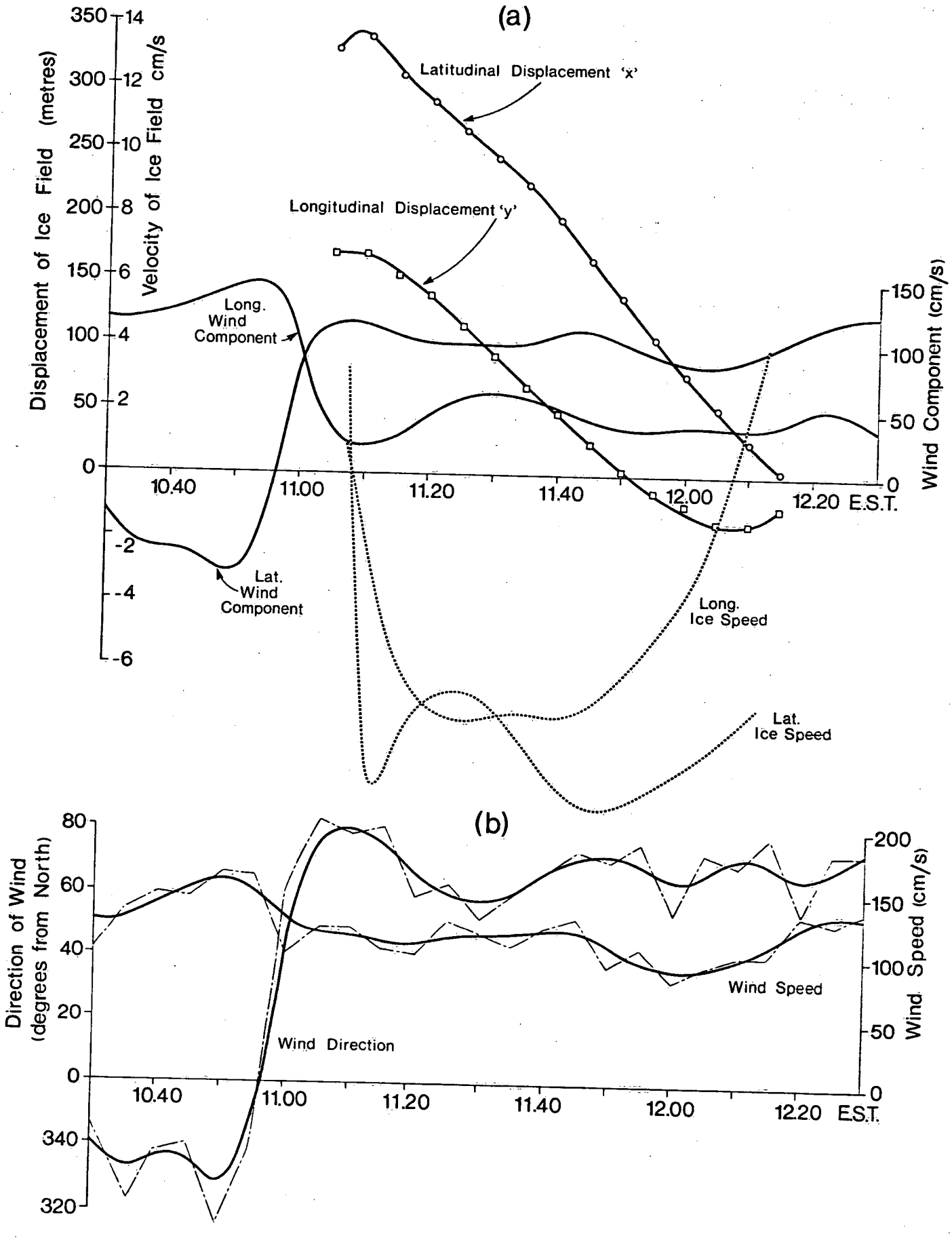

Fig.4 Displacement and Velocity of the Ice Field and the Associated Wind

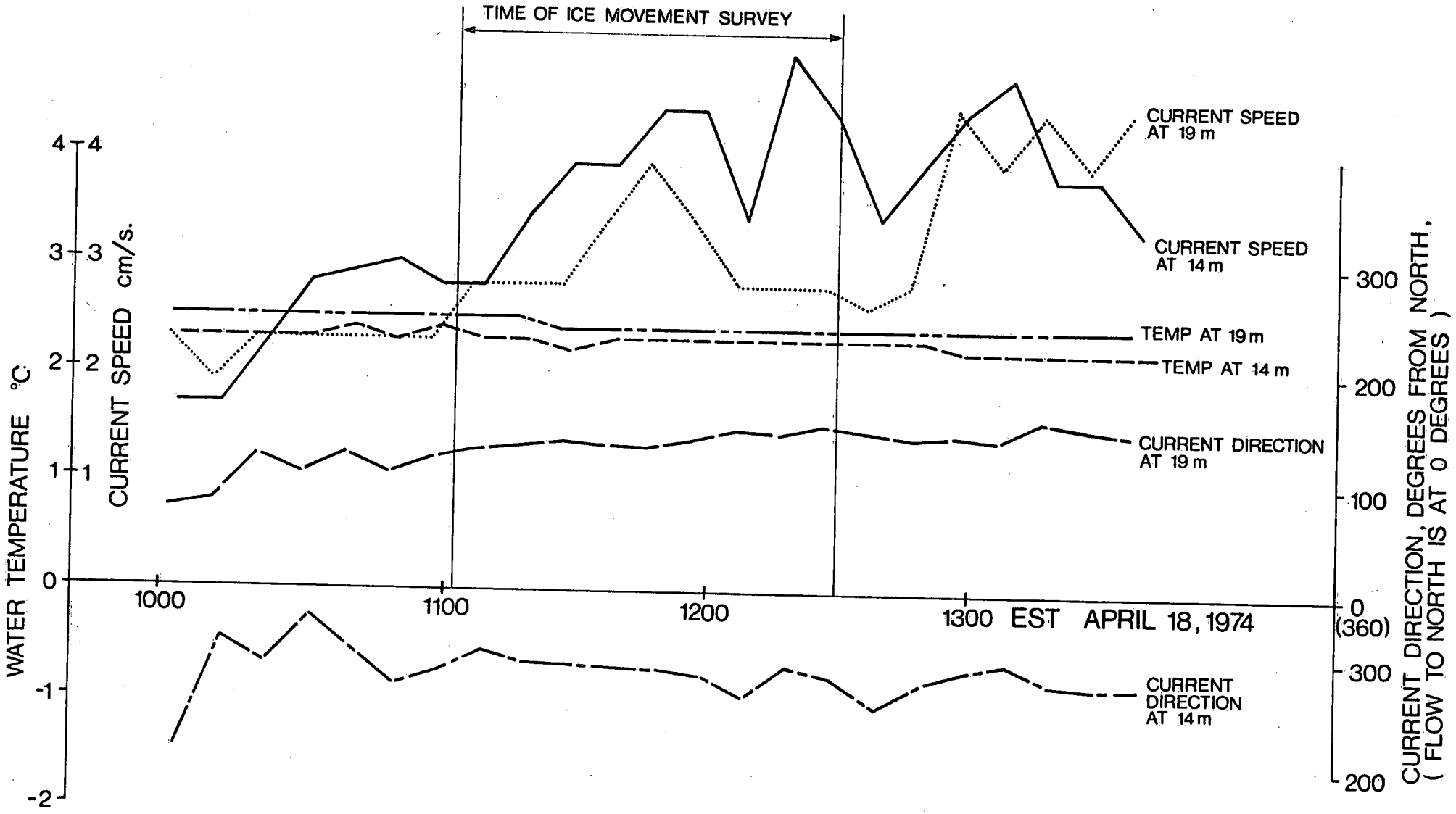

FIG. 5 LIMNOLOGICAL DATA AT TIME OF ICE MOVEMENT

Table 1. Measured Values of ϕ and ψ

Time:	1104	1112	1117	1122	1127
ϕ :	57°04'17"	59°23'24"	62°11'23"	66°38'02"	73°25'32"
	1133	1140	1145	1151	1156
	82°44'57"	97°04'14"	110°22'37"	125°39'02"	138°41'39"
	1204	1210	1215	after 1215	
	154°08'46"	163°47'43"	171°42'48"	out of sight	
Time:	1108	1120	1125	1130	1135
ϕ:	36°56'00"	38°31'20"	40°26'00"	43°32'20"	47°08'00"
	1143	1147	1154	1159	1207
	52°52'30"	59°00'05"	68°14'40"	80°46'20"	104°54'05"
	1213	1217	1223	1226	1229
	132°07'20"	154°51'55"	171°13'00"	176°42'00"	181°28'30"
	1234	after 1234			
	185°50'30"	out of sight			

Note: - Time shown is Eastern Standard Time (E.S.T.).

Table 2: Comparison of Roughness Lengths and Wind Drag Coefficients by different Researchers.

Researcher Year	Method of Analysis	$C_{D,10}$	z_o cm	Remarks
Untersteiner and Badgley, 1965	Logarithmic wind profile analysis	0.7×10^{-3} (Calculated from z_o on the right, not given in the original paper)	Scattered over 3 orders of magnitude. Logarithmic average 0.02	1. Measured over Arctic sea ice floes. 2. Ice surface smooth with shallow snow cover or melt water ponds.
Suzuki, 1966	Logarithmic wind profile analysis and direct wind shear measurement	1.35×10^{-3} (see above)	0.0025 - 0.02	1. Measured over a flat sea ice bordering the shore in a harbour. 2. The Von Karman constant was treated as an unknown. Its experimental value varied from 0.43 to 0.70.
Smith, Banke and Johannessen, 1970	Turbulence correlation analysis	Neutral stability: $(1.1\text{-}1.4) \times 10^{-3}$ Average 1.3×10^{-3} Unstable stability: $(1.7\text{-}2.0) \times 10^{-3}$ Average 1.85×10^{-3}	Neutral Stability: 0.22 - 0.48 Average 0.35 Unstable Stability: 0.97 - 1.49 Average 1.14	1. Measured over packed sea ice with 80-90% coverage. 2. Ice floes were soft and slushy with no directional characteristics. Snow cover 30-50 cm. 3. Stability was determined by the Richardson number. when $\lvert R_i \rvert < 0.03$, wind neutrally stable when $R_i < -0.03$, wind unstable
Banke and Smith, 1971	Turbulence correlation analysis	Stable stability: $(1.14\text{-}1.44) \times 10^{-3}$ Average 1.3×10^{-3}	Stable stability: 0.228 - 0.569 Average 0.33	1. Measured over packed sea ice with 75% coverage. 2. Ridges up to 1 m above ice surface. Average height of ridges 30 cm. Ridges randomly distributed.
Smith, 1972	Turbulence correlation analysis	Mean value for all stability conditions: $(0.7 \pm 0.15) \times 10^{-3}$	-	1. Measured over a large drifting ice floe. 2. The ice surface was smooth and with snow cover.
Seifert and Langleben, 1972	Logarithmic wind profile analysis	Smoother site: 0.85×10^{-3} (median) rougher site: 1.1×10^{-3} (median)	Smoother Site: 0.002 - 0.15 Rougher Site: 0.05 - 0.40	1. Measured over packed sea ice with 90-95% coverage. 2. Ice 20 - 30 cm thick, snow and slush up to 12 cm. 3. There was no ridge and rafting. 4. Measurements were made over two sites with visible roughness difference. 5. Wind profile for $\lvert R_i \rvert < 0.03$ were used in the analysis.
Langleben, 1972	Logarithmic wind profile analysis	Smooth ice floe: $(0.83 \pm 0.04) \times 10^{-3}$ and $(0.85 \pm 0.05) \times 10^{-3}$ Rough ice floe: $(1.21 \pm 0.03) \times 10^{-3}$ and $(1.23 \pm 0.02) \times 10^{-3}$	Smooth ice floe: 0.051 and 0.053 Rough ice floe: 0.28 and 0.30	1. Measurements were made at junction of two Arctic ice floes. 2. The smoother ice floe was flat, unbroken and with light snow cover up to 5 cm. 3. The rougher ice floe was heavily rafted with surface irregularities up to 1 m high. Pressure ridges were randomly distributed both in orientation and spacing. The typical spacing is of the order of 1 km. 4. The wind profile was assumed to be completely effected by the upwind floe.
Banke and Smith, 1973	Turbulence correlation analysis	Beaufort Sea: $(0.475\text{-}1.095) \times 10^{-3}$ Arctic Ocean: $(0.705\text{-}1.19) \times 10^{-3}$ Robeson Channel: $(0.78\text{-}1.26) \times 10^{-3}$	Beaufort Sea: 0.041 Arctic Ocean: 0.076 Robeson Channel: 0.145	1. Measurements were made at Beaufort Sea, Arctic Ocean and Robeson Channel. 2. All data were analysed together regardless of stability.
Study Reported here	Ice field movement measurement and wind analysis	3.26×10^{-3}	0.0824	1. Measured over fresh water ice on a lake. 2. Ice field had a coverage close to 100%. 3. Extensive telescoping and ridging in the ice field, mostly less than 50 cm high. 4. Wind blew perpendicular to the ridges and telescoping lines.